Introduction

Several minimally-invasive, easy-to-use cancer diagnostic methods using peripheral blood or urine samples have recently been developed to ease the physical burden on patients and to reduce the costs and time involved [1,2,3,4,5,6,7,8]. Rapid advances have been made in cancer diagnosis and prognosis methods based on metabolome analysis [3,9,10,11,12,13,14], which frequently involves the use of multivariate analysis techniques, such as computer-aided, machine-learning systems for data mining.

Although metabolome analysis is a promising approach in screening for diseases such as cancer, some practical limitations remain. These include the necessity to measure a huge number of metabolites [15,16,17], data-redundancy problems, including the false-discovery rate (FDR) and overfitting, and cost constraints. One approach to overcoming these problems is "focused metabolomics", which limits the objects of the analysis to those that play roles in general metabolism and share physical similarities.

Amino acids are among the most suitable candidates for focused metabolomics as they are either ingested or synthesized endogenously and play essential physiological roles both as basic metabolites and metabolic regulators. To measure amino acids, plasma free amino acids (PFAAs), which abundantly circulate as a medium linking all organ systems, would be the most favorable target because their profiles have been known to be influenced by metabolic variations in specific organ systems induced by specific diseases [18,19,20,21]. Additionally, plasma samples can be collected easily from patients.

Several investigators have also reported changes in PFAA profiles in cancer patients [22,23,24,25,26,27,28]. However, despite evidence of a relationship between PFAA profiles and some types of cancer, few studies have explored the use of PFAA profiles for diagnosis because, although PFAA profiles differ significantly between patients, the differences in individual amino acids do not always provide sufficient discrimination abilities by themselves [24,29,30]. To address this issue, we previously constructed and tested a diagnostic index based on PFAA concentrations, known as the "AminoIndex technology" [29,30,31,32,33], to compress multidimensional information from PFAA profiles into single dimension and maximize the differences between patients and controls (Figure 1). We obtained preliminary data on the efficacy of the "AminoIndex technology" for the early detection of colorectal, breast, and lung cancers in approximately 150 samples from a single medical institute [29,30].

Moreover, technologies have recently been developed to analyze amino acids with high accuracy. For example, we developed a method to measure PFAA profiles using high-performance liquid chromatography (HPLC)–electrospray ionization (ESI)–mass spectrometry (MS) [34,35,36].

The present study aimed to determine the possibility of PFAA profiling for cancer diagnosis using a large number of samples from multiple medical institutes. We measured the PFAA profiles of approximately 200 cancer patients from three different institutes each with one of the following five types of cancer: lung, gastric, colorectal (CRC), breast, or prostate cancer. Patients were compared to five times sizes of gender- and age-matched controls also used in this study. We then compared the alterations in the

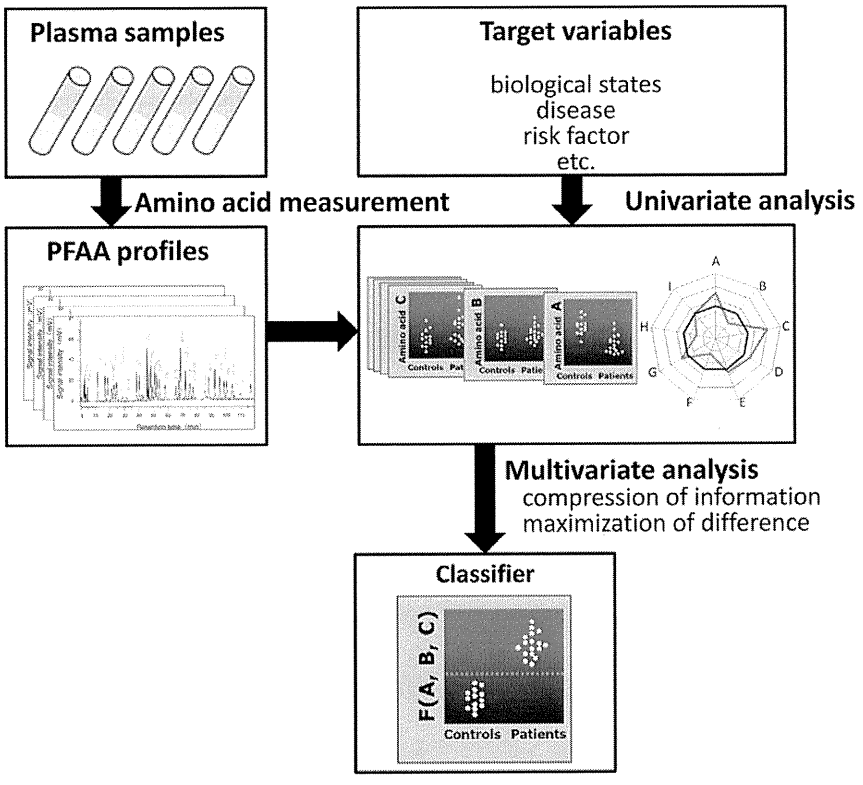

Figure 1. Concept of the generation of "AminoIndex technology". At the top of the diagram, PFAA concentrations are measured for each subject. In the middle, target variables and univariate analysis of PFAA profiles are represented. At the bottom, an estimation of the classifier with optimized discriminating power using multivariate analysis is presented.
doi:10.1371/journal.pone.0024143.g001

PFAA profiles between the cancer patients and the controls using univariate and multivariate analyses. As a result, significant alterations in PFAA profiles were observed in cancer patients in comparison to control subjects. We demonstrated two types of alterations in PFAA profiles in cancer patients: some differences reflected the metabolic changes common to many cancers, while others were specific to each type of cancer. We also found that both common and cancer type-specific alterations in PFAA profiles were observed even in the patients with early stage cancer. Furthermore, using a large number of samples allowed us to verify the robustness of PFAA profiling for the early detection of various cancers.

Materials and Methods

Ethics

The study was conducted in accordance with the Declaration of Helsinki, and the protocol was approved by the ethics committees of the Kanagawa Cancer Center, the Osaka Medical Center for Cancer and Cardiovascular Diseases, the Okayama University Hospital, the Yokohama City University Medical Center, the Gunma Prefectural Cancer Center, the Shizuoka Prefectural Cancer Center, the Chiba Prefectural Cancer Center, the Yokohama Municipal Citizen's Hospital, the Yokohama Minami Kyosai Hospital, the Kanagawa Health Service Association, the Kameda Medical Center Makuhari, and the Mitsui Memorial Hospital. All subjects gave their written informed consent for inclusion before they participated in the study. All data were analyzed anonymously throughout the study.

Subjects

Data from Japanese patients with lung cancer (LC), gastric cancer (GC), colorectal cancer (CRC), breast cancer (BC), and prostate cancer (PC) were analyzed in this study. The patients had been histologically diagnosed with primary cancer at various Japanese medical institutes between 2006 and 2009. The LC patients were recruited from the Osaka Medical Center for Cancer and Cardiovascular Diseases, the Chiba Prefectural Cancer Center, the Kanagawa Cancer Center, and the Gunma Prefectural Cancer Center. The GC patients were recruited from the Okayama University Hospital, the Gunma Prefectural Cancer Center, and the Shizuoka Prefectural Cancer Center. The CRC patients were recruited from the Kanagawa Cancer Center, the Shizuoka Prefectural Cancer Center, and the Gunma Prefectural Cancer Center. The BC patients were recruited from the Yokohama City University Medical Center, the Kanagawa Cancer Center, and the Gunma Prefectural Cancer Center. The PC patients were recruited from the Kanagawa Cancer Center, the Yokohama Municipal Citizen's Hospital, the Yokohama Minami Kyosai Hospital, and the Gunma Prefectural Cancer Center. Control subjects with no apparent cancer were chosen from among those undergoing comprehensive medical examinations at three different Japanese medical institutes (the Center for Multiphasic Health Testing and Services of the Mitsui Memorial Hospital, the Kameda Medical Center Makuhari, and the Kanagawa Health Service Association) between 2008 and 2009.

Colonic polyp patients were recruited from among those undergoing endoscopic polypectomy at the Kameda Medical Center Makuhari between 2006 and 2008.

For the purposes of data analysis, the patients were assigned to five groups based on their primary cancer diagnoses (~140–200 patients per group), and five age- and gender-matched control groups were also established (Table 1). Data sets for all of the cancer patients and controls, as well as all cancer patients stratified by gender, were also analyzed.

PFAA measurement

Blood samples were collected from the controls and the patients prior to any medical treatment. Blood samples (5 ml) were collected from forearm veins after overnight fasting in tubes containing ethylenediaminetetraacetic acid (EDTA; Termo, Tokyo, Japan) and were immediately placed on ice. Plasma was prepared by centrifugation at 3,000 rpm at 4°C for 15 min and then stored at −80°C until analysis. After the plasma collection, all samples were stored and processed at the Institute for Innovation of the Ajinomoto Co., Inc. (Kawasaki, Japan). To reduce any bias

Table 1. Demographic and clinical characteristics of subjects.

Data set		LC		GC		CRC		BC		PC	
		Patients	Controls	Patients	Controls	Patients	Controls	Patients	Controls	Patients	Controls
Size	Total	200	996	199	985	199	995	196	976	134	666
	M/F	125/75	635/371	126/73	626/359	114/85	570/425	0/196	0/976	134/0	666/0
Age	Mean	65.0[a]	63.2	64.8[a]	62.9	63.7	62.4	55.3	54.5	69.4[c]	65.8
	(SD)	(10.0)	(9.2)	(10.8)	(9.7)	(9.5)	(9.5)	(12.6)	(11.1)	(6.7)	(6.1)
BMI	Mean	22.5	22.9	22.7	22.8	23.0	22.8	22.4	22.0	23.4	23.4
	(SD)	(3.8)	(3.0)	(3.2)	(3.0)	(3.7)	(3.0)	(3.4)	(3.5)	(2.7)	(2.5)
Stage	0	-		-		8		26	-	-	
	I(A)	29		120		63		75		0	
	II(B)	16		29		48		73		95	
	III(C)	54		26		59		13		19	
	IV(D)	28		24		19		0		15	
	Uncharacterized	1		0		2		9		5	

[a]$p<0.05$,
[c]$p<0.001$.
For LC, GC, CRC, and BC, cancer stages were determined according to the International Union Against Cancer TNM Classification of Malignant Tumors, 6th edition [38], and for PC, cancer stages were determined according to Jewett staging system [39].
doi:10.1371/journal.pone.0024143.t001

introduced prior to analysis, samples were analyzed in random order. The plasma samples were deproteinized using acetonitrile at a final concentration of 80% before measurement. The amino-acid concentrations in the plasma were measured by HPLC–ESI–MS, followed by precolumn derivatization. The analytical methods used were as described previously [34,35,36].

Among the 20 genetically-encoded amino acids, glutamate (Glu), aspartate (Asp), and cysteine (Cys) were excluded from the analysis because they are unstable in blood. Citrulline (Cit) and ornithine (Orn) were measured instead because they are relatively abundant in blood and are known to play important roles in metabolism. The following 19 amino acids and related molecules were therefore measured and analyzed: alanine (Ala), arginine (Arg), asparagine (Asn), Cit, glutamine (Gln), glycine (Gly), histidine (His), isoleucine (Ile), leucine (Leu), lysine (Lys), methionine (Met), Orn, phenylalanine (Phe), proline (Pro), serine (Ser), threonine (Thr), tryptophan (Trp), tyrosine (Tyr), and valine (Val).

Two metrics were made for each of the 19 amino acids including the absolute concentration of each amino acid, which directly reflected its availability and consumption, and the ratios associated with the specific metabolic status in each organ. The concentrations of the amino acids in the plasma were expressed in μM, and the ratios of the amino acid concentrations were expressed by the follow equation:

$$X2_{i,j} = \frac{X_{i,j}}{\sum_k X_{i,k}}$$

where $X2_{i,j}$ is ratio of the amino-acid concentration of the j-th amino acid of i-th subject, and $X_{i,j}$ is the plasma concentration (μM) of the j-th amino acid of i-th subject.

Statistical analysis

Two types of metric were used for each data set for analysis using either the amino-acid concentration or the ratio as explanatory variables.

Mean and SD. The mean amino-acid concentrations ± standard deviations (SDs) were calculated to determine summarized PFAA profiles for both patients and controls.

Mann-Whitney U-test. The Mann-Whitney *U*-test was used to assess significant differences of the plasma amino-acid concentrations between the patients and the controls.

ROC analysis. Receiver-operator characteristic (ROC) curve analyses were performed to determine the abilities of uni- and multi-variate analyses to discriminate between patients and controls. The patient labels were fixed as positive class labels. Therefore, an area under the ROC curve (AUC of ROC) value of <0.5 indicated that the amino acid level was lower in the patients than the controls, whereas an AUC of ROC value of >0.5 indicated that it was higher. The 95% confidence interval (95% CI) of AUC of ROC for the discrimination of patients based on amino acid concentrations and ratios was also estimated as described by Hanley and McNeil [37].

Two-way analysis of variance (ANOVA). The two-way ANOVA was used to evaluate the effects of gender, age, and smoking status as potential confounding factors. The presence of cancer and gender were assumed to be independent factors, age was treated as a continuous predictor rather than a categorical predictor, and the interaction term between the presence of cancer and smoking status was analyzed.

Two-class linear discrimination analysis (LDA). Linear discrimination analysis (LDA) with stepwise variable selection was performed to distinguish patients with each type of cancer from the control subjects, in which both the maximum and the minimum p-values for a term to be added or removed were set at 0.001.

Multi-class LDA for discrimination. LDA with stepwise variable selection was also performed to distinguish patients with a specific cancer from the complete data set containing all cancer patients stratified by gender (four kinds of cancer patients in each data set). Because the size of each group was smaller than that of two-class LDA, the maximum p-value for a term to be added was set at 0.05 and the minimum p-value for a term to be removed was set at 0.10. The Mahalanobis distance was used as a metric of classification. The accuracy was defined as the ratio of the correctly discriminated patients to the total number of patients with each cancer instead of AUC of ROC because ROC analysis could be applied only for two-class discrimination.

Leave one out cross—validation (LOOCV). LOOCV was performed to correct potential over-optimization for obtained LDA models. Briefly, one sample was omitted from the study data set, and the LDA model was calculated for the remaining samples to estimate coefficients for each amino acid. The function values for the left-out sample were calculated based on the model. This process was repeated until every sample in the study data set had been left out once.

Conditional logistic-regression (c-logistic) analysis. C-logistic analysis was also performed to verify the effects of age and gender, potential confounding factors, on the discriminatory abilities of obtained LDA models to differentiate patients with each type of cancer from the controls.

Subgroup analysis. To assess the effects of cancer stage, each data set was divided into a sub-data set according to disease stage and including corresponding controls, and analyzed using the ROC analysis in each data set.

Software

MATLAB (The Mathworks, Natick, MA) was used for the calculations of mean and SD, the Mann-Whitney *U*-test, ROC analysis, two-way ANOVA, LDAs, and LOOCV. GraphPad Prism (GraphPad Software, La Jolla, CA) was also used for the ROC curve analysis. LogXact (Cytel, Cambridge, MA) was used for the c-logistic analysis.

Results

Characteristics of subjects

Table 1 summarizes the characteristics of the subjects in this study. The data sets comprised 200 LC patients and 996 controls, 199 GC patients and 985 controls, 199 CRC patients and 995 controls, 198 BC patients and 976 controls, and 134 PC patients and 666 controls (Table 1). The sample size for each cancer type was greater than those in previous reports [25] and provided sufficient statistical power to test the robustness of the PFAA profiles for cancer diagnosis.

There were no significant differences in body mass index (BMI) among the data sets (Table 1). Weight loss due to malnutrition was therefore not expected to influence the results. Although significant differences in average age were observed among the data sets (LC, $p<0.05$; GC, $p<0.05$; and PC, $p<0.001$), the effects appeared to be relatively minor because the absolute values of these differences were small (Table 1).

For LC, GC, CRC, and BC, disease stages were determined according to the Sixth Edition of the International Union Against Cancer (UICC) Tumor–Node–Metastasis (TNM) Classification of Malignant Tumors [38]. For PC, the stage was determined

according to the Jewett staging system [39]. For all types of cancer, a large proportion of the patients had early-stage disease. The fractions of patients at each stage according to type of cancer were as follows: ~50% stage I, ~10% stage II, ~25% stage III, and ~15% stage IV for LC; ~60% stage I, ~15% stage II, ~13% stage III, and ~12% stage IV for GC; ~35% stages 0 and I, ~25% stage II, ~30% stage IV, and ~10% stage IV for CRC; ~5% stage 0, ~25% stage I, ~25% stage II, and ~7% stage III for BC; and ~75% stage B, ~13% stage C, and ~12% stage D for PC (Table 1).

The patients with each type of cancer could be further subdivided based on histological type (for LC, GC, CRC, and BC) or Gleason score (for PC), as is summarized in Table S1. The characteristics of 34 colonic polyp patients as well as the smoking status of patients are also summarized in Table S1.

Shared PFAA profiles among cancers

Univariate analysis was used to compare the PFAA profiles of the cancer patients and controls. The differences in the significance levels of each amino acid between the patients and the controls are shown in Figure 2A. The results of the ROC analysis are depicted in Figure 2B because the levels of significance depend on sample size. The concentrations and ratios of each amino acid profile for both patients and controls are shown in Tables S2. And the AUCs of ROC and their CIs of each amino acid are shown in Table S3 (concentration) and Table S4 (ratio), respectively.

Two-way ANOVA was used to evaluate the potential confounding effects of gender, age, and smoking status. Correcting for these factors did not greatly affect the significance levels of each amino acid, suggesting that their effects on the PFAA profiles were minor (Table S5).

The plasma concentrations of Gln, Trp, and His were significantly decreased in all of the cancers except PC, and none of the amino acids showed increased concentrations across all types of cancer ($p<0.05$). The ratios of Trp and His were significantly decreased, while those of Pro and Orn were increased, in all cancers ($p<0.05$) (Figure 2).

To further examine the shared traits among cancer patients, the PFAA profiles were compared using a pooled data set including all cancer patients and controls. Notably, the amino acids that were affected by this type of analysis had significant differences in both concentration and ratio: 11 amino acids (Asn, Gln, Cit, Val, Met, Leu, Tyr, Phe, His, Trp, and Arg) showed decreases, while four amino acids (Ser, Pro, Gly, and Orn) exhibited increases (Figure 2). Changes in Gln, Trp, His, Pro, and Orn were detected in the analysis for all types of cancer. Alterations in these amino acids might therefore reflect characteristic changes in metabolism that are common to all cancers.

Specific PFAA profiles for each cancer

In addition to the changes that were common to all of the cancers, we detected alterations in PFAA profiles that were specific to each disease type (Figure 2). Overall, the concentrations of most amino acids were decreased in GC and CRC patients, whereas no clear trends in amino acid concentrations were observed in the other groups (Figure 2). Furthermore, some of the amino acids showed opposite trends in different types of cancer. For example, the concentrations of Thr were decreased in GC and CRC patients, but increased in BC patients (Figure 2). These variations in the PFAA profiles might reflect specific characteristics of each cancer, in contrast to the limited set of amino acids that are responsible for the metabolic changes shared by all cancers.

Changes in PFAA profiles in early-stage cancers

Although alterations in the PFAA profiles of cachexic patients with advanced cancer have been well documented, few reports have considered early-stage patients. However, a large fraction of the cancer patients in the current data set were in the early stages of disease (Table 1). The differences in PFAA profiles according to disease stage were therefore examined for each cancer (Figure 3, Figure S1, Table S3, Table S4).

Notably, alterations in the PFAA profiles were detected in all patients, including those in the early stages of disease, in the current study. All amino-acid concentrations and ratios were drastically decreased in early stage disease patients, regardless of the subsequent progression. In particular, significant decreases of each amino acid concentration were observed in GC and CRC patients (Figure 3A), and changes in each ratio were notable in all of the cancer patients (Figure 3B).

Early-stage cancer patients are generally asymptomatic. Moreover, most of the subjects in the present study did not show significant weight loss (a symptom typical of cachectic patients) (Table 1), anorexia, or decreases in serum albumin concentrations (data not shown). The changes in the PFAA profiles in cancer patients therefore appeared to be independent of any effects caused by poor nutrition resulting from tumor progression.

Discriminating cancer patients and controls by PFAA profiles

The results of the univariate analyses suggested that cancer patients and controls could be discriminated using multivariate analysis. By assuming that the presence of cancer and the concentrations or ratios of the PFAA profiles were objective and explanatory variables, respectively, LDA was able to distinguish cancer patients from the corresponding controls with variable selection. The results of variable selection are indicated in Table 2 (concentration) and Table S6 (ratio), respectively.

The discrimination abilities for each cancer patient were evaluated using the AUC of ROC of the discriminate score and were found to be >0.75 in all cases (Table 3 and Table S7). In concrete analysis, AUCs for the discrimination of patients based on the amino acid concentrations and ratios, respectively, were also estimated as follows: 0.802 (95% CI: 0.766~0.838) and 0.802 (95% CI: 0.767~0.837) for LC; 0.849 (95% CI: 0.816~0.882) and 0.816 (95% CI: 0.780~0.852) for GC; 0.874 (95% CI: 0.842~0.906) and 0.881 (95% CI: 0.851~0.910) for CRC; 0.778 (95% CI: 0.741~0.815) and 0.778 (95% CI: 0.741~0.815) for BC; and 0.783 (95% CI: 0.740~0.826) and 0.779 (95% CI: 0.740~0.819) for PC (Table 3 and Table S7). The discriminate analysis was therefore able to adequately distinguish between different types of patient cancer.

Variable selection was also performed for each cancer patient. Eight amino acids were selected in more than two of the five kinds of cancers: Gln, Ala, Val, Ile, His, Trp, Orn, and Lys for the concentrations (Table 2A); and Ser, Gln, Val, Met, His, Trp, Lys, and Arg for the ratios (Table S6). Four of the amino acids (Gln, Val, His, and Trp) among each set were selected for both explanatory variables (Table 2 and Table S6). These amino acids were similar to those associated with all types of cancer as indicated by the univariate analysis (Gln, Trp, His, Pro, and Orn).

On the other hand, some amino acids incorporated into the LDA model were not identified as significant amino acids by the univariate analysis. For example, the Val concentration did not show a significant alteration in the univariate analysis (Figure 2A), but it was incorporated into the LDA model (Table 2). Because plasma concentrations of each amino acid are metabolically connected to each other, there might be a potential correlation that cannot be

A

Concentration

Amino acid	LC	GC	CRC	BC	PC	Pooled
Thr						
Ser						
Asn						
Gln						
Pro						
Gly						
Ala						
Cit						
Val						
Met						
Ile						
Leu						
Tyr						
Phe						
His						
Trp						
Orn						
Lys						
Arg						

Ratio

Amino acid	LC	GC	CRC	BC	PC	Pooled
Thr						
Ser						
Asn						
Gln						
Pro						
Gly						
Ala						
Cit						
Val						
Met						
Ile						
Leu						
Tyr						
Phe						
His						
Trp						
Orn						
Lys						
Arg						

B

Concentration

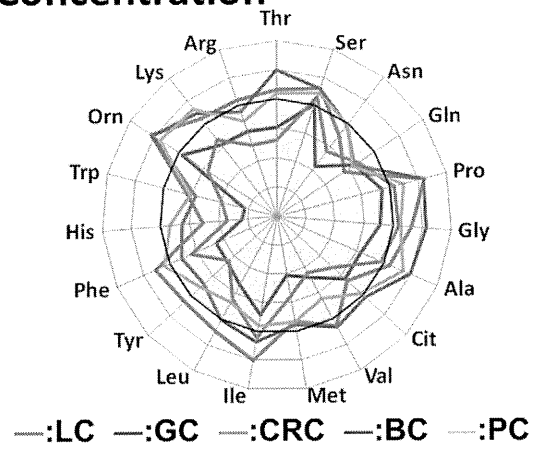

Pooled data

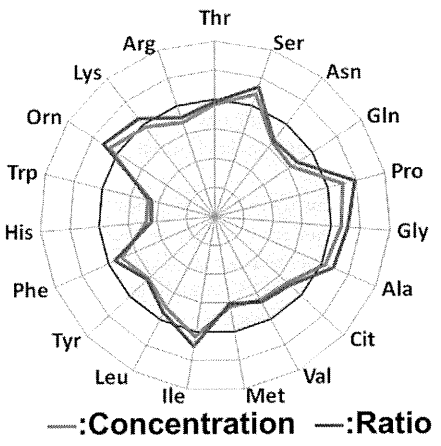

Ratio

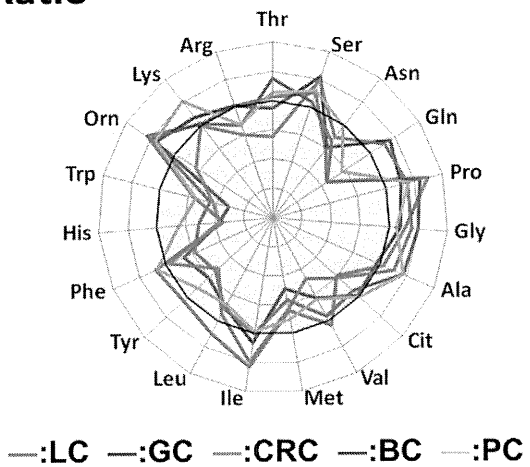

Scale of AUC of ROC

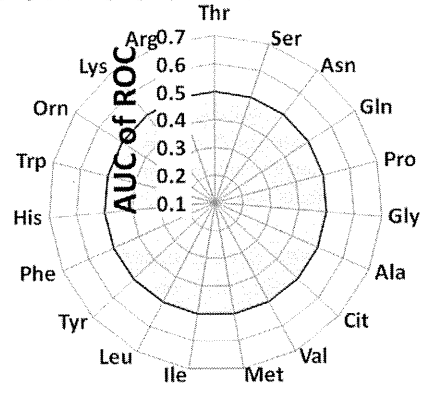

Figure 2. PFAA profiles of cancer patients. The results of the Mann-Whitney *U*-test (A) and receiver-operator characteristic (ROC) curve analysis (B) are indicated. A. Colored cells indicate that the concentration or ratio is increased in cancer patients at $p<0.001$ (red), $p<0.01$ (orange), and $p<0.05$ (pink), and decreased in cancer patients at $p<0.001$ (blue), $p<0.01$(sky blue), and $p<0.05$ (light blue), respectively. B. Axes show the AUC of ROC for each amino acid to discriminate patients from controls. Concentrations and ratios of each cancer patient and the pooled data set are indicated, respectively. Black bold lines indicate the point where the AUC of ROC = 0.5.
doi:10.1371/journal.pone.0024143.g002

detected by the univariate analysis alone. Indeed, Spearman's partial correlation coefficient between Val and cancer (or not) was −0.127 ($p<0.001$), while the correlation coefficient between these two factors was 0.035 (not significant). Therefore, this suggested that the obtained LDA model reflected the metabolic network of PFAAs, which were not apparent thorough univariate analysis.

Because the obtained results may have been over-optimized, LOOCV was carried out to generate an unbiased analysis. This produced AUCs similar to those obtained for LDA, suggesting that there was no obvious over-optimization in the obtained LDA models (Table 3 and Table S7).

Subgroup analyses of divided data sets according to cancer stage, including corresponding controls, were then performed to assess the ability of PFAA profiles to distinguish between stages of cancer for each type of disease. In any stage of each cancer, the AUC of ROC was found to be higher than 0.75, suggesting that the obtained LDA models would thus be expected to be effective in detecting early as well as advanced stage cancers (Table 3 and Table S7).

The discrimination abilities for all cancer patients were also evaluated. The AUCs of ROC for both concentrations and ratios were 0.796 (95% CI: 0.779~0.814) and 0.785 (95% CI: 0.767~0.803), respectively (Table 3 and Table S7). Notably, most of the 19 amino acids were statistically selected for these discriminations: 16 for the concentrations and 12 for the ratios. Even using a rough classification, regardless of the type of cancer, it was possible to discriminate between patients and controls with high accuracy, and the overall contributions of numerous amino acids might reflect the large-scale characteristic changes associated with cancer metabolism.

A c-logistic analysis using matching factors (gender and age) was performed for each data set to evaluate and correct for potential confounding factors. Note that we used the combinations of amino acids obtained from the LDA models as explanatory variables. Although the c-logistic analysis was performed using all of the significant variables identified by the univariate analysis, the amino acids identified in the LDA were utilized to correct for potential confounding factors more adequately (data not shown). Both the levels of significance (Table 2 and Table S6) and the discrimination abilities (Table 3 and Table S7) were not significantly altered by correcting for the potentially confounding factors, suggesting that these results were independent of gender and age effects.

To evaluate patients with non-neoplastic diseases, the PFAA profiles of colonic polyp patients were substituted into the LDA model for CRC. Most of the colonic polyp patients (31/34, 91.2%) were classified into the control group for the concentrations and ratios of both models, suggesting that the obtained models could discriminate CRC patients specifically.

Discrimination between cancer types by PFAA profiles

In addition to differentiating between patients with each type of cancer and the controls, discrimination among patients within each cancer group was also performed by separating all the cancer patients into each disease subtype according to gender. This was done because the results of the present analyses identified changes in PFAA profiles that were common to all types of cancer as well as those specific to individual cancers.

The accuracies of all discriminant analyses using amino acid concentrations as explanatory variables were close to or better than 50% both in male patients (Table 4) and female patients (Table 5) data set. The discrimination accuracy among cancer patients was less than that between patients and controls. Six amino acids (Gly, Cit, Val, Tyr, Trp, and Arg) were commonly selected in these analyses, regardless of gender (data not shown). An additional six amino acids (Gln, Met, Leu, His, Orn, and Lys) were selected in the male patient data set, and four (Thr, Ser, Ile, and Phe) were selected in the female patient data set (data not shown). Five of the 16 amino acids listed above were selected in the discrimination between patients and controls, while the remainder might have been responsible for the characteristic features of each cancer.

The accuracies were similar between the analyses using ratios as explanatory variables and those using concentrations both in male patients (Table S8) and female patients (Table S9). Seven amino acids (Gln, Cit, Val, Tyr, Trp, Lys, and Arg) were commonly selected regardless of gender in these analyses (data not shown). An additional four amino acids (Ala, Met, Leu, and His) were selected in the male patient data set, and four (Thr, Ser, Ile, Orn) were selected in the female patient data set (data not shown). Five amino acids (Cit, Val, Tyr, Trp, and Arg) from each set were selected for both explanatory variables, suggesting that the changes to the respective PFAAs were specific to certain types of cancer.

LOOCV was also carried out and resulted in similar accuracies for the discrimination analyses, suggesting that there was no obvious over-optimization in the obtained models (Table 4, Table 5, Table S8 and Table S9).

Discussion

The present study demonstrated the use of PFAA profiling as a focused metabolomics approach for the early detection of patients with any of five types of cancer. Combining novel analytical techniques and both univariate and multivariate statistical analyses, previously unknown aspects of amino acid metabolism in humans have been revealed. The sample size in the present study was considerably larger than those reported previously [25,29,30], and provided sufficient statistical power to test the robustness of PFAA profiling for cancer diagnosis. We also demonstrated the possibility of detecting cancers, both specifically and broadly, using multivariate analysis to compress the PFAA profile data, even for patients with early stage cancer.

In the previous studies, the alterations in PFAA profiles in cancer patients sometimes seem inconsistent[22,23,24,25,26,27,28,29,30], and some discrepancies existed between our current study and those reported in the literature [25]. This discrepancy may be due not only to sample size and the varying predominance of early stage cancers but also to some other factors such as amino acid measurement methods. On the other hand, alterations in the PFAA profiles in our present study were consistent with the results of our previous studies, in which samples were collected from a single medical institute [29,30]. Furthermore, there are also many similarities between our results and those of previous studies. For example, decreases in His and Gln levels, which have been observed broadly in previous reports, and increases in Pro and Ala levels in BC are consistent with our findings [25].

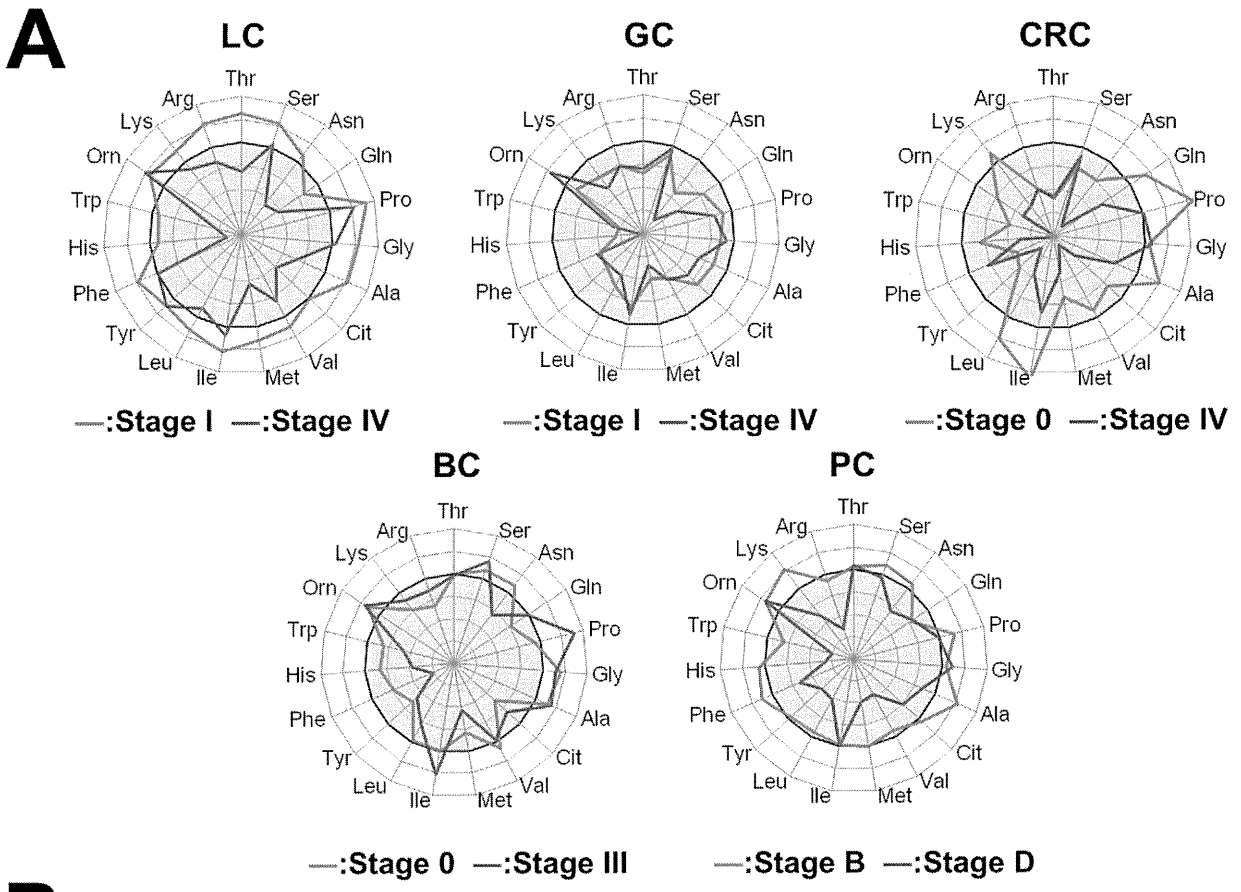
A
LC
GC
CRC
Thr
Ser
Asn
Gln
Pro
Gly
Ala
Cit
Val
Met
Ile
Leu
Tyr
Phe
His
Trp
Orn
Lys
Arg
—:Stage I —:Stage IV
—:Stage I —:Stage IV
—:Stage 0 —:Stage IV
BC
PC
—:Stage 0 —:Stage III
—:Stage B —:Stage D

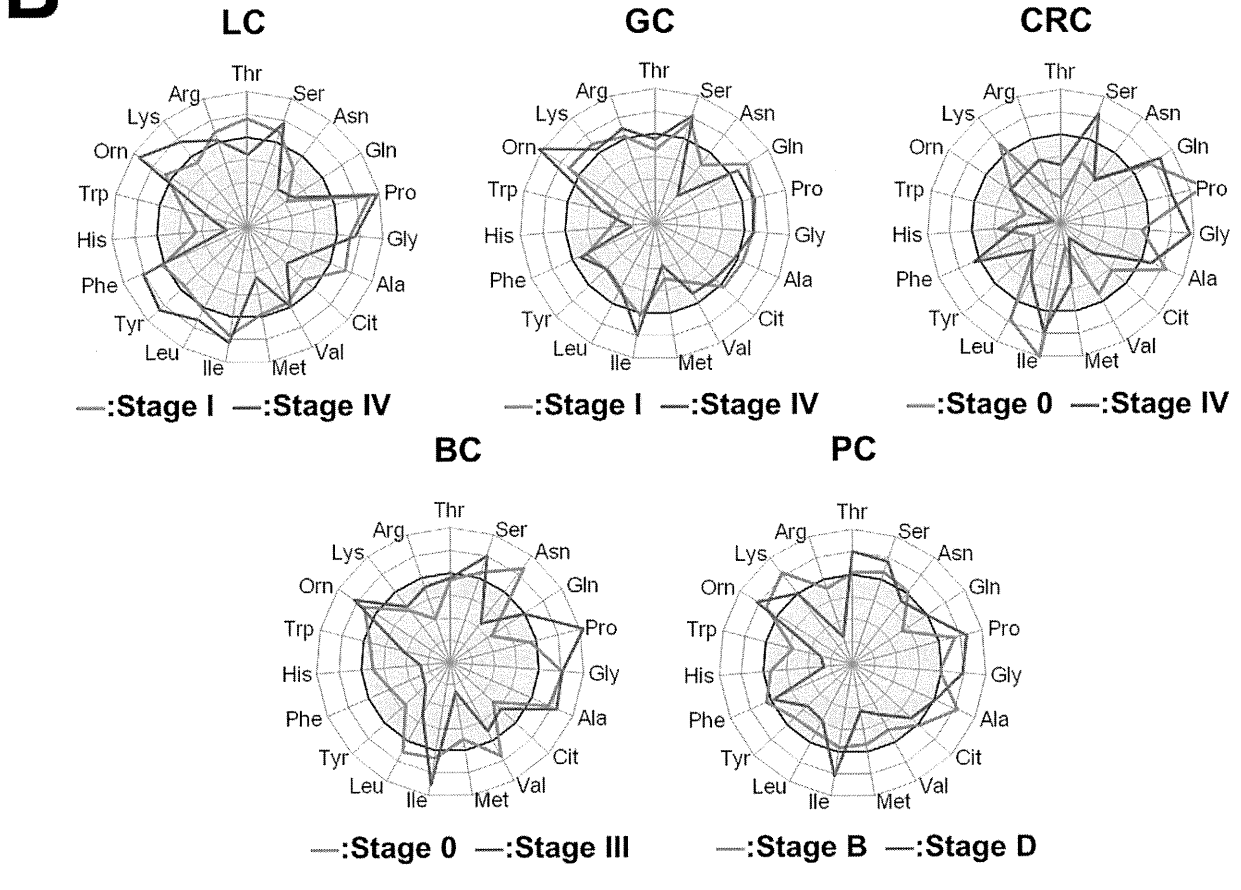
B
LC
GC
CRC
Thr
Ser
Asn
Gln
Pro
Gly
Ala
Cit
Val
Met
Ile
Leu
Tyr
Phe
His
Trp
Orn
Lys
Arg
—:Stage I —:Stage IV
—:Stage I —:Stage IV
—:Stage 0 —:Stage IV
BC
PC
—:Stage 0 —:Stage III
—:Stage B —:Stage D

Figure 3. PFAA profiles of early- and advanced-stage cancer patients. The axes show the AUC of ROC for each amino acid for discriminating patients from controls. A. Comparison of concentrations of cancer patients and controls. B. Comparison of ratios of cancer patients and controls. Scale as described for Figure 2. For LC, GC, CRC, and BC, cancer stages were determined according to the International Union Against Cancer TNM Classification of Malignant Tumors, 6th edition [38], and for PC, cancer stages were determined according to Jewett staging system [39].
doi:10.1371/journal.pone.0024143.g003

Cancer is expected to become the leading cause of death worldwide within a few years. Therefore, it is crucial that methods for the prevention, early detection, and treatment of cancers should be implemented to reduce mortality. Various screening methods have been established for the cancers included in our study. However, the high specificity of these methods means that subjects must undergo each screening examination separately, which can be expensive and time consuming. These examinations can also impose a physical and/or mental burden upon subjects, which can lead to avoidance. By contrast, the method described in the present study involves a relatively simple plasma assay and imposes a low physical burden on subjects. This method could also be used as versatile health assessment as other diseases in which PFAA profiles can be altered, such as diabetes[18], hepatic failure[19], and renal failure[21], can also be evaluated.

It should be noted that the models derived from this case-control study could not be used directly to make further observations or predictions, despite providing a preliminary demonstration of the potentially high value of this method for cancer discrimination. Further investigations, including model construction and validation using cohorts with larger sample sizes, are in progress to clarify the clinical utility of this approach. Moreover, the possibility of continuous PFAA profiling as a means to determine prognosis after surgery or chemotherapy is also being investigated.

Our investigation demonstrated two types of alterations in PFAA profiles of cancer patients: those in a limited set of amino acids reflecting metabolic changes common to many cancers; and those in a larger group of amino acids representing metabolic characteristics specific to each cancer. Alterations in PFAA profiles were observed even in patients with early-stage cancer, most of whom had no apparent symptoms. This strongly suggested that the alterations in PFAA profiles identified in the current study were independent of the effects of poor nutrition caused by tumor progression.

Many previous reports have shown that metabolism, including that of amino acids, is notably altered in cancer cells [3,13,40] and that changes in PFAA profiles can also occur [22,24,25,26,27,28,29,30], especially in cachexic patients with advanced cancer [23,25]. Among whole metabolites, amino acids have been frequently identified as having associations with cancer in other studies [10,13,41,42,43]. The current study demonstrated that mechanisms other than malnutrition can drive the changes in PFAA profiles.

Besides cancer-dependent malnutrition, significant decreases in PFAA concentrations and various indicators of nutritional status such as BMI and serum albumin levels are observed in cancer-independent cachexia [44,45,46]. In the present study, no apparent decreases in those indicators were observed, strongly suggesting that alterations in PFAA were also independent of nutritional status mediated by factors not related to cancer.

Table 2. Variables incorporated into LDA and c-logistic models using concentrations as explanatory variables.

Amino acid	LC		GC		CRC		BC		PC		Pooled	
	LDA	C-logit	LDA	C-logit	LDA	C-logit	LDA	C-logit	LDA	C-logit	LDA	C-logit
Thr							+++	+++			+++	+++
Ser	+++	+++			+++	+++					+++	+++
Asn												
Gln	−−−	−−−					−−−	−−−	−−−	−−−	−−−	−−−
Pro	+++	+++									+++	+++
Gly							+++	++				
Ala					+++	+++	+++	+++	+++	+++	+++	+++
Cit	−−−	−−−	−−−	−							−−−	
Val	−−−	−	−−−	−−	−−−	−−−			−−−	−−−	−−−	−−−
Met											−−−	−−−
Ile	+++	+++	+++	+	+++	+++			+++	++	+++	+++
Leu					+++	+++					+++	++
Tyr					−−−	−−−	−−−	−−				
Phe	+++	+++									+++	+++
His	−−−	−−−	−−−	−−−	−−−	−−−					−−−	−−−
Trp	−−−	−−−	−−−	−−−	−−−	−−	−−−	−−−	−−−	−−−	−−−	−−−
Orn	+++	+++					+++	+++	+++	+++	+++	+++
Lys			+++	+++	+++	+++			+++	+++	+++	+++
Arg					−−−	−−−			−−−	−−−	−−−	−−−

+, ++, +++: positive coefficients in the model.
−, −−, −−−: negative coefficients in the model.
+,−: $p<0.05$, ++,−−: $p<0.01$, +++,−−−: $p<0.001$.
doi:10.1371/journal.pone.0024143.t002

Table 3. Discrimination performance of LDA and c-logistic models using concentrations as explanatory variables.

Model	Subjects		LC	GC	CRC	BC	PC	Pooled
LDA	All	AUC	0.802	0.849	0.874	0.778	0.783	0.796
		CI	(0.766~0.836)	(0.816~0.882)	(0.842~0.906)	(0.741~0.815)	(0.740~0.826)	(0.779~0.814)
	LOOCV	AUC	0.792	0.845	0.868	0.769	0.767	0.793
	Stage 0 patients	AUC	-	-	0.903	0.813		
		CI			(0.807~1.00)	(0.726~0.900)		
	Stage I patients	AUC	0.752	0.859	0.859	0.754		
		CI	(0.698~0.805)	(0.820~0.898)	(0.800~0.918)	(0.692~0.817)		
	Stage II(B) patients	AUC	0.870	0.829	0.921	0.786	0.764	
		CI	(0.772~0.969)	(0.726~0.933)	(0.877~0.954)	(0.727~0.847)	(0.710~0.819)	
	Stage III(C) patients	AUC	0.844	0.834	0.817	0.755	0.777	
		CI	(0.780~0.908)	(0.748~0.920)	(0.743~0.892)	(0.621~0.889)	(0.669~0.885)	
	Stage IV(D) patients	AUC	0.901	0.843	0.950	-	0.873	
		CI	(0.837~0.966)	(0.734~0.951)	(0.895~1.00)		(0.771~0.974)	
C-logit	All	AUC	0.806	0.850	0.876	0.776	0.786	0.798
		CI	(0.771~0.841)	(0.816~0.883)	(0.845~0.907)	(0.739~0.812)	(0.743~0.829)	(0.780~0.815)

doi:10.1371/journal.pone.0024143.t003

Nevertheless, it remains unclear how the metabolic changes occurring in cancer patients affect the PFAA profile of the whole body, even in patients with early-stage tumors. To clarify the relationship between carcinogenesis and changes in PFAA profiles, we are further investigating the contribution of local effects caused by cancer cell metabolism and the systemic responses of the immune system against tumors or factors released by cancer cells.

Changes in metabolism can be detected in cancer cells even in early-stage patients. Hirayama *et al.* reported no significant correlation between the levels of cancer cell metabolites, including several amino acids, and the tumor stage [13]. The metabolism of Trp is of particular interest because it was identified as one of the most important amino acids in relation to cancer progression in our study. Overexpression of indoleamine-2,3- dioxygenase (IDO), the first enzyme in the kynurenine Trp metabolism pathway in humans, has been reported in cancer cells [47]. IDO is induced in many different tumors and has been suggested to play a role in cancer-mediated evasion of the immune system [47,48,49,50].

Arg, Orn, Cit, and Pro are known to be closely related to immune function. For example, Qiu *et al.* reported an association between the urea cycle and metabolic alterations in CRC patients and found no correlation between the metabolite profile and cancer progression [43]. Cancer cells also release factors that can alter general physical conditions. For example, the transcriptional regulatory molecule high-mobility group B1 (HMGB1) was recently shown to regulate cancer-cell tumorigenesis, expansion, and invasion [51,52,53].

Further elucidation of these mechanisms might allow for the development of both static and dynamic models of carcinogenesis through system analysis [31]. Recently, computer-aided studies have been reported that integrate hierarchical 'omics' datasets for the systemic understanding of metabolic phenotypes to reconstruct the regulatory network from physiological data by means of system analysis. System analysis of cancer patients based on whole body amino acid metabolism could reveal information concerning the nature of a disease and help to establish strategies for its prevention, early detection, prognosis, monitoring, and treatment.

In contrast to many similar efforts to detect biomarkers of disease as single specific molecules (DNA, microRNA, proteins, peptides, or metabolites) in peripheral blood, our approach was to focus on the metabolic status, which is indicative of multivariate function, using non-specific metabolites. Therefore, we believe that our method is superior to those used in other studies, both in versatility and efficiency, because only one amino acid measurement can be applied for detection of various disease states (i.e., renal failure, hepatic failure, and nutritional status).

Table 4. Multiclass discriminant analyses of male cancer patients using concentrations as explanatory variables.

		Patients with:			
		LC	GC	CRC	PC
Discriminated as:	LC	**72(69)**	*19(22)*	*12(13)*	*26(26)*
	GC	*18(19)*	**58(52)**	*16(17)*	*25(25)*
	CRC	*13(14)*	*25(28)*	**71(69)**	*16(17)*
	PC	*22(23)*	*24(24)*	*15(15)*	**67(66)**
	Total	125	126	114	134
	Accuracy	**57.6%(55.2%)**	**46.0%(41.3%)**	**62.3%(60.5%)**	**50.0%(49.3%)**

The numbers in the blanket indicate the results of LOOCV.

doi:10.1371/journal.pone.0024143.t004

Table 5. Multiclass discriminant analyses of female cancer patients using concentrations as explanatory variables.

		Patients with:			
		LC	**GC**	**CRC**	**BC**
Discriminated as:	LC	**41(37)**	*4(6)*	*8(11)*	*43(44)*
	GC	*13(14)*	**40(38)**	*15(16)*	*30(30)*
	CRC	*6(8)*	*13(13)*	**52(47)**	*17(17)*
	BC	*15(16)*	*16(16)*	*10(11)*	**106(105)**
	Total	75	73	85	196
	Accuracy	**54.7%(49.3%)**	**54.8%(52.1%)**	**61.2%(55.2%)**	**54.1(53.6%)**

The numbers in the blanket indicate the results of LOOCV.
doi:10.1371/journal.pone.0024143.t005

Supporting Information

Figure S1 PFAA profiles of cancer patients stratified by progression stage. The axes show the AUC of ROC for each amino acid for discriminating patients from controls. A. Comparison of concentrations of cancer patients and controls. B. Comparison of ratios of cancer patients and controls. Scale as described for Figure 2. For LC, GC, CRC, and BC, cancer stages were determined according to the International Union Against Cancer TNM Classification of Malignant Tumors, 6th edition [38], and for PC, cancer stages were determined according to Jewett staging system [39].
(TIF)

Table S1 Detailed demographic and clinical characteristics of subjects. a: $p<0.05$, c: $p<0.001$ *: For LC, GC, CRC, and BC, cancer stages were determined according to the International Union Against Cancer TNM Classification of Malignant Tumors, 6th edition [38], and for PC, cancer stages were determined according to Jewett staging system [39].
(XLS)

Table S2 PFAA profiles of cancer patients and controls.
(XLS)

Table S3 AUCs of ROC of each amino acid concentration for discrimination for cancer patients from controls.
(XLS)

Table S4 AUCs of ROC of each amino acid ratio for discrimination for cancer patients from controls. AUCs were calculated using all patients and controls, and patiens and matched controls stratified by cancer stage.
(XLS)

Table S5 Significance values for PFAA profiles for each data set by two-way ANOVA for the effects of cancer existence and other parameters. Column headings indicate Mann-Whitney U-test of cancer existence (None), two-way ANOVA for the effects of cancer existence and gender (Gender), cancer existence and age (Age), and cancer existence and smoking status (Smoking).
(XLS)

Table S6 Variables incorporated into LDA and c-logistic models using ratios as explanatory variables. +, ++, +++: positive coefficients in the model −, −−, −−−: negative coefficients in the model +,−: $p<0.05$, ++,−−: $p<0.01$, +++,−−−: $p<0.001$.
(XLS)

Table S7 Discrimination performance of LDA and c-logistic models using ratios as explanatory variables.
(XLS)

Table S8 Multiclass discriminant analyses of male cancer patients using ratios as explanatory variables. The numbers in the blanket indicate the results of LOOCV.
(XLS)

Table S9 Multiclass discriminant analyses of female cancer patients using ratios as explanatory variables. The numbers in the blanket indicate the results of LOOCV.
(XLS)

Acknowledgments

We thank Mr. Takashi Yamamoto and Ms. Naoko Kageyama for the amino acid analysis, Dr. Takashi Daimon for help with the statistical analysis, and Ms. Mariko Takasu and Ms. Tomoko Kasakura for help with data acquisition. We also thank all members of the medical staffs of the Osaka Medical Center for Cancer and Cardiovascular Diseases, the Chiba Prefectural Cancer Center, the Kanagawa Cancer Center, the Okayama University Hospital, the Shizuoka Prefectural Cancer Center, the Gunma Prefectural Cancer Center, Yokohama City University Medical Center, the Yokohama Municipal Citizen's Hospital, the Yokohama Minami Kyosai Hospital, the Center for Multiphasic Health Testing and Services of the Mitsui Memorial Hospital, the Kameda Medical Center Makuhari, and the Kanagawa Health Service Association for help with sample collection.

Author Contributions

Conceived and designed the experiments: YM HY MY NO. Performed the experiments: MH AG MA TI T. Miura NS EB HK FI MM II AC FO HM OT T. Mitsushima MY NO. Analyzed the data: YM AI KH. Contributed reagents/materials/analysis tools: HM. Wrote the paper: YM AI KH.

References

1. Couzin J (2009) Biomarkers. Metabolite in urine may point to high-risk prostate cancer. Science 323: 865.
2. Hunter MP, Ismail N, Zhang X, Aguda BD, Lee EJ, et al. (2008) Detection of microRNA expression in human peripheral blood microvesicles. PLoS One 3: e3694.
3. Kim Y, Koo I, Jung BH, Chung BC, Lee D (2010) Multivariate classification of urine metabolome profiles for breast cancer diagnosis. BMC Bioinformatics 11 Suppl 2: S4.
4. Nevedomskaya E, Ramautar R, Derks R, Westbroek I, Zondag G, et al. (2010) CE-MS for metabolic profiling of volume-limited urine samples: application to accelerated aging TTD mice. J Proteome Res 9: 4869–4874.
5. Pasikanti KK, Esuvaranathan K, Ho PC, Mahendran R, Kamaraj R, et al. (2010) Noninvasive urinary metabonomic diagnosis of human bladder cancer. J Proteome Res 9: 2988–2995.

6. Tiziani S, Lopes V, Gunther UL (2009) Early stage diagnosis of oral cancer using 1H NMR-based metabolomics. Neoplasia 11: 269–276, 264p following 269.
7. Roth C, Kasimir-Bauer S, Pantel K, Schwarzenbach H (2011) Screening for circulating nucleic acids and caspase activity in the peripheral blood as potential diagnostic tools in lung cancer. Mol Oncol 5: 281–291.
8. Roth C, Rack B, Muller V, Janni W, Pantel K, et al. (2010) Circulating microRNAs as blood-based markers for patients with primary and metastatic breast cancer. Breast Cancer Res 12: R90.
9. Abate-Shen C, Shen MM (2009) Diagnostics: The prostate-cancer metabolome. Nature 457: 799–800.
10. Asiago VM, Alvarado LZ, Shanaiah N, Gowda GA, Owusu-Sarfo K, et al. (2010) Early detection of recurrent breast cancer using metabolite profiling. Cancer Res 70: 8309–8318.
11. Bictash M, Ebbels TM, Chan Q, Loo RL, Yap IK, et al. (2010) Opening up the "Black Box": metabolic phenotyping and metabolome-wide association studies in epidemiology. J Clin Epidemiol 63: 970–979.
12. Chadeau-Hyam M, Ebbels TM, Brown IJ, Chan Q, Stamler J, et al. (2010) Metabolic profiling and the metabolome-wide association study: significance level for biomarker identification. J Proteome Res 9: 4620–4627.
13. Hirayama A, Kami K, Sugimoto M, Sugawara M, Toki N, et al. (2009) Quantitative metabolome profiling of colon and stomach cancer microenvironment by capillary electrophoresis time-of-flight mass spectrometry. Cancer Res 69: 4918–4925.
14. Slupsky CM, Steed H, Wells TH, Dabbs K, Schepansky A, et al. (2010) Urine metabolite analysis offers potential early diagnosis of ovarian and breast cancers. Clin Cancer Res 16: 5835–5841.
15. Blaise BJ, Shintu L, Elena B, Emsley L, Dumas ME, et al. (2009) Statistical recoupling prior to significance testing in nuclear magnetic resonance based metabonomics. Anal Chem 81: 6242–6251.
16. Denkert C, Budczies J, Kind T, Weichert W, Tablack P, et al. (2006) Mass spectrometry-based metabolic profiling reveals different metabolite patterns in invasive ovarian carcinomas and ovarian borderline tumors. Cancer Res 66: 10795–10804.
17. Rubtsov DV, Waterman C, Currie RA, Waterfield C, Salazar JD, et al. (2010) Application of a Bayesian deconvolution approach for high-resolution (1)H NMR spectra to assessing the metabolic effects of acute phenobarbital exposure in liver tissue. Anal Chem 82: 4479–4485.
18. Felig P, Marliss E, Ohman JL, Cahill CF, Jr. (1970) Plasma amino acid levels in diabetic ketoacidosis. Diabetes 19: 727–728.
19. Fischer JE, Rosen HM, Ebeid AM, James JH, Keane JM, et al. (1976) The effect of normalization of plasma amino acids on hepatic encephalopathy in man. Surgery 80: 77–91.
20. Holm E, Sedlaczek O, Grips E (1999) Amino acid metabolism in liver disease. Curr Opin Clin Nutr Metab Care 2: 47–53.
21. Hong SY, Yang DH, Chang SK (1998) The relationship between plasma homocysteine and amino acid concentrations in patients with end-stage renal disease. J Ren Nutr 8: 34–39.
22. Cascino A, Muscaritoli M, Cangiano C, Conversano L, Laviano A, et al. (1995) Plasma amino acid imbalance in patients with lung and breast cancer. Anticancer Res 15: 507–510.
23. Heber D, Byerly LO, Chlebowski RT (1985) Metabolic abnormalities in the cancer patient. Cancer 55: 225–229.
24. Kubota A, Meguid MM, Hitch DC (1992) Amino acid profiles correlate diagnostically with organ site in three kinds of malignant tumors. Cancer 69: 2343–2348.
25. Lai HS, Lee JC, Lee PH, Wang ST, Chen WJ (2005) Plasma free amino acid profile in cancer patients. Semin Cancer Biol 15: 267–276.
26. Norton JA, Gorschboth CM, Wesley RA, Burt ME, Brennan MF (1985) Fasting plasma amino acid levels in cancer patients. Cancer 56: 1181–1186.
27. Proenza AM, Oliver J, Palou A, Roca P (2003) Breast and lung cancer are associated with a decrease in blood cell amino acid content. J Nutr Biochem 14: 133–138.
28. Vissers YL, Dejong CH, Luiking YC, Fearon KC, von Meyenfeldt MF, et al. (2005) Plasma arginine concentrations are reduced in cancer patients: evidence for arginine deficiency? Am J Clin Nutr 81: 1142–1146.
29. Maeda J, Higashiyama M, Imaizumi A, Nakayama T, Yamamoto H, et al. (2010) Possibility of multivariate function composed of plasma amino acid profiles as a novel screening index for non-small cell lung cancer: a case control study. BMC Cancer 10: 690.
30. Okamoto N, Miyagi Y, Chiba A, Akaike M, Shiozawa M, et al. (2009) Diagnostic modeling with differences in plasma amino acid profiles between non-cachectic colorectal/breast cancer patients and healthy individuals. Int J Med Med Sci 1: 1–8.
31. Kimura T, Noguchi Y, Shikata N, Takahashi M (2009) Plasma amino acid analysis for diagnosis and amino acid-based metabolic networks. Curr Opin Clin Nutr Metab Care 12: 49–53.
32. Noguchi Y, Zhang QW, Sugimoto T, Furuhata Y, Sakai R, et al. (2006) Network analysis of plasma and tissue amino acids and the generation of an amino index for potential diagnostic use. Am J Clin Nutr 83: 513S–519S.
33. Zhang Q, Takahashi M, Noguchi Y, Sugimoto T, Kimura T, et al. (2006) Plasma amino acid profiles applied for diagnosis of advanced liver fibrosis in patients with chronic hepatitis C infection. Hepatol Res 34: 170–177.
34. Shimbo K, Kubo S, Harada Y, Oonuki T, Yokokura T, et al. (2009) Automated precolumn derivatization system for analyzing physiological amino acids by liquid chromatography/mass spectrometry. Biomed Chromatogr 24: 683–691.
35. Shimbo K, Oonuki T, Yahashi A, Hirayama K, Miyano H (2009) Precolumn derivatization reagents for high-speed analysis of amines and amino acids in biological fluid using liquid chromatography/electrospray ionization tandem mass spectrometry. Rapid Commun Mass Spectrom 23: 1483–1492.
36. Shimbo K, Yahashi A, Hirayama K, Nakazawa M, Miyano H (2009) Multifunctional and highly sensitive precolumn reagents for amino acids in liquid chromatography/tandem mass spectrometry. Anal Chem 81: 5172–5179.
37. Hanley JA, McNeil BJ (1982) The meaning and use of the area under a receiver operating characteristic (ROC) curve. Radiology 143: 29–36.
38. Sobin L, Wittekind C, eds. TNM Classification of Malignant Tumours, Sixth Edition. New York: Wiley-Liss.
39. Jewett HJ (1975) The present status of radical prostatectomy for stages A and B prostatic cancer. Urol Clin North Am 2: 105–124.
40. Borgan E, Sitter B, Lingjaerde OC, Johnsen H, Lundgren S, et al. (2010) Merging transcriptomics and metabolomics - advances in breast cancer profiling. BMC Cancer 10: 628.
41. Rocha CM, Barros AS, Gil AM, Goodfellow BJ, Humpfer E, et al. (2010) Metabolic profiling of human lung cancer tissue by 1H high resolution magic angle spinning (HRMAS) NMR spectroscopy. J Proteome Res 9: 319–332.
42. Urayama S, Zou W, Brooks K, Tolstikov V (2010) Comprehensive mass spectrometry based metabolic profiling of blood plasma reveals potent discriminatory classifiers of pancreatic cancer. Rapid Commun Mass Spectrom 24: 613–620.
43. Qiu Y, Cai G, Su M, Chen T, Zheng X, et al. (2009) Serum metabolite profiling of human colorectal cancer using GC-TOFMS and UPLC-QTOFMS. J Proteome Res 8: 4844–4850.
44. Bossola M, Tazza L, Luciani G (2009) Mechanisms and treatment of anorexia in end-stage renal disease patients on hemodialysis. J Ren Nutr 19: 2–9.
45. Morrison WL, Gibson JN, Rennie MJ (1988) Skeletal muscle and whole body protein turnover in cardiac cachexia: influence of branched-chain amino acid administration. Eur J Clin Invest 18: 648–654.
46. Polge A, Bancel E, Bellet H, Strubel D, Poirey S, et al. (1997) Plasma amino acid concentrations in elderly patients with protein energy malnutrition. Age Ageing 26: 457–462.
47. Lob S, Konigsrainer A, Zieker D, Brucher BL, Rammensee HG, et al. (2009) IDO1 and IDO2 are expressed in human tumors: levo- but not dextro-1-methyl tryptophan inhibits tryptophan catabolism. Cancer Immunol Immunother 58: 153–157.
48. Lob S, Konigsrainer A, Rammensee HG, Opelz G, Terness P (2009) Inhibitors of indoleamine-2,3-dioxygenase for cancer therapy: can we see the wood for the trees? Nat Rev Cancer 9: 445–452.
49. Muller AJ, DuHadaway JB, Donover PS, Sutanto-Ward E, Prendergast GC (2005) Inhibition of indoleamine 2,3-dioxygenase, an immunoregulatory target of the cancer suppression gene Bin1, potentiates cancer chemotherapy. Nat Med 11: 312–319.
50. Zamanakou M, Germenis AE, Karanikas V (2007) Tumor immune escape mediated by indoleamine 2,3-dioxygenase. Immunol Lett 111: 69–75.
51. Chung HW, Lee SG, Kim H, Hong DJ, Chung JB, et al. (2009) Serum high mobility group box-1 (HMGB1) is closely associated with the clinical and pathologic features of gastric cancer. J Transl Med 7: 38.
52. Lotze MT, DeMarco RA (2003) Dealing with death: HMGB1 as a novel target for cancer therapy. Curr Opin Investig Drugs 4: 1405–1409.
53. Sims GP, Rowe DC, Rietdijk ST, Herbst R, Coyle AJ (2010) HMGB1 and RAGE in inflammation and cancer. Annu Rev Immunol 28: 367–388.

Zhou et al. BMC Systems Biology 2011, 5(Suppl 1):S16
http://www.biomedcentral.com/1752-0509/5/S1/S16

BMC Systems Biology

REPORT Open Access

Network screening of Goto-Kakizaki rat liver microarray data during diabetic progression

Huarong Zhou[1*], Shigeru Saito[2,3], Guanying Piao[1,4], Zhi-Ping Liu[1], Jiguang Wang[1], Katsuhisa Horimoto[2,5*], Luonan Chen[1,2,5*]

From The 4th International Conference on Computational Systems Biology (ISB 2010)
Suzhou, P. R. China. 9-11 September 2010

Abstract

Background: Type 2 diabetes mellitus (T2DM) is a complex systemic disease, with significant disorders of metabolism. The liver, a central energy metabolic organ, plays a critical role in the development of diabetes. Although gene expression levels are able to be measured via microarray since 1996, it is difficult to evaluate the contributions of one altered gene expression to a specific disease. One of the reasons is that a whole network picture responsible for a specific phase of diabetes is missing, while a single gene has to be put into a network picture to evaluate its importance. In the aim of identifying significant transcriptional regulatory networks in the liver contributing to diabetes, we have performed comprehensive active regulatory network survey by network screening in 4 weeks (w), 8-12 w, and 18-20 w Goto-Kakizaki (GK) rat liver microarray data.

Results: We identify active regulatory networks in GK rat by network screening in the following procedure. First, the regulatory networks are compiled by using the known binary relationships between the transcriptional factors and their regulated genes and the biological classification scheme, and second, the consistency of each regulatory network with the microarray data measured in GK rat is estimated to detect the active networks under the corresponding conditions. The comprehensive survey of the consistency between the networks and the measured data by the network screening approach in the case of non-insulin dependent diabetes in the GK rat reveals: 1. More pathways are active during inter-middle stage diabetes; 2. Inflammation, hypoxia, increased apoptosis, decreased proliferation, and altered metabolism are characteristics and display as early as 4weeks in GK strain; 3. Diabetes progression accompanies insults and compensations; 4. Nuclear receptors work in concert to maintain normal glycemic robustness system.

Conclusion: Notably this is the first comprehensive network screening study of non-insulin dependent diabetes in the GK rat based on high throughput data of the liver. Several important pathways have been revealed playing critical roles in the diabetes progression. Our findings also implicate that network screening is able to help us understand complex disease such as diabetes, and demonstrate the power of network systems biology approach to elucidate the essential mechanisms which would escape conventional single gene-based analysis.

* Correspondence: hrzhou@sibs.ac.cn; k.horimoto@aist.go.jp; lnchen@sibs.ac.cn
[1]Key Laboratory of Systems Biology, SIBS-Novo Nordisk Translational Research Centre for PreDiabetes, Shanghai Institutes for Biological Sciences, Chinese Academy of Sciences, Shanghai 200233, China
[2]Computational Biology Research Center, National Institute of Advanced Industrial Science and Technology, Tokyo 135-0064, Japan
Full list of author information is available at the end of the article

Background

The globe figure of people with diabetics is increasing rapidly [1]. The diabetes epidemic worldwide is due to an interaction between environment and genetic risk factors [2]. The modern environment causes diabetes in many ways, such as stress, increased availability of unhealthy food, and decreased physical activities [3]. Our body system is a robustness system to keep our blood glucose within normal ranges with various perturbations. However, in genetically susceptible individuals, long term unfavorable environmental factors will affect epigenetics, thereafter gene expressions, and eventually lead to diabetes. T2DM is chronic with nature history lasting for more than twenty years, which has been divided into five stages: latent stage, transition stage, impaired glucose tolerance stage (IGT), impaired fasting glucose stage (IFT), and overt stage [4]. IGT and IFT stages are called prediabetes. During the first 4 stages, the sub-health status is still able to return to normals. Once reached stage 5, overt stage, T2DM is diagnosed. The systems of diabetes are also robust: even with food restriction, increased physical activity, and multidrug therapies, diseases are usually impossible to return back to normals [5].

In order to detailed study diabetes, several animal models have been developed. Goto-Kakizaki (GK) rat, a spontaneous non insulin dependent diabetes model with a heterogeneous background, is recognized as one of the best model for human T2DM. The colony was first produced in Japan by selective repeated inbreeding nondiabetic Wistar-Kyoto (WKY) rats with minor glucose intolerance [6]. The diabetic state became spontaneous and stable after 30 generations. The characteristics of GK subcolonies are slightly different. However the important hallmarks are the same, including inherent decreased beta cell mass, moderate hyperglycemia, insulin resistance, and a non-obese phenotype [7]. At embryonic day 16, beta cell mass of GK rats is only 50% of that in normal WKY controls. GK fetuses show decreased insulin levels and decreased beta cell mass. Before 2 weeks of age, GK babies show normal blood glucose, but decreased insulin levels. Basal hyperglycemia has been detected at 3-4 weeks. GK rats show unstable blood glucose levels between 6-12 weeks and hyperglycemia became consistent in GK rats older than 18 weeks of age. Although it exhibits similar metabolic disorders to the human diabetes, GK is non obese without hyperlipidemia at the beginning. Thus it only represents a subset of human T2DM.

T2DM is a systemic metabolic disease. The two major characters are insulin resistance and beta cells fail to compensate. Liver plays a key role in not only energy metabolism but also insulin resistance, thus liver gene expression changes play a role in the progression of diabetes. Now most scientists agree that the risk of developing T2DM is low with only single gene mutation [8]. Environmental factors act on predisposing individuals, changing their DNA modification and mRNA expression to certain levels until the system is not able to return to normals. Microarray technology makes it easy and accurate to measure significantly changed gene expressions [9,10]. However, to understand the real meaningful hints from the information ocean and to elucidate the connections between changed biological molecules and diseases seem quite challenge.

It has been recognized that a complex disease cannot be fully understood by merely analyzing individual genes or biomolecules. It is interactions or networks of those components that are ultimately responsible for malfunctions of the system. Therefore, instead of picking up single interesting gene, we are using network screening to analyze the active networks or pathways based on the high throughput data, a promising approach to investigate associations between biological molecules and phenotypes. A knowledge-based network is constructed first by extracting as many relationships identified by experimental studies as possible and then superimposing them to microarray data. Recently, we proposes a method [11] to estimate the consistency of a given network with the measured data: i) the network is quantified into a log-likelihood from the measured data, based on the Gaussian network, and ii) the probability of the likelihood corresponding to the measured data, named the graph consistency probability (GCP), is estimated based on the generalized extreme value distribution. In this paper, we survey the active regulatory networks in GK and WKY rats liver in a comprehensive manner by network screening. The microarray data measured previously for five liver samples of both groups at each of 5 time points [12] are analyzed by the standard statistical techniques and the network screening. The analyses reveal the expression signatures different between GK and WKY rats and the network signatures that are composed of the networks well consistent between the network structure and the graph structure. As a result, we present the candidates of active regulatory networks, which including new and reasonable networks, as well as the networks previously reported as to be essential to diabetes. Furthermore, we discuss merits and pitfalls of the present approach for surveying the active regulatory networks for a special disease.

Materials and Methods

• Network Screening

Overview

The candidates of active regulatory networks are detected by network screening in the following manner. First, the regulatory network sets are generated by

combining the binary relationships between transcriptional factors (TFs) and their regulating genes, which are compiled in TRANSFAC database [13], and the functional gene sets defined in the Molecular Signatures Database (MSigDB) [14]. Then, we calculate the graph consistency probability (GCP) [11], which expresses the consistency of a given network structure with the monitored expression data of the constituent genes in this study, for each of the network structures obtained at the first step. In addition, in each reference network, the enrichment probability of the genes with the significant differences between GK and WKY rats (expression signature) is further tested. For this purpose, the expression signature is determined using the Student's t-test (for a false discovery rate [FDR] < 5% in expression between GK and WKY rats). The number of genes included in the expression signature is tested for each network, based on the hyper-geometric probability. Thus, we refine the candidates of active regulatory networks, in terms of both the network structure by GCP and the extent of gene expression by enrichment probability. The significance of both thresholds is set to 0.05. The details of the reference network and the GCP are described, below.

Reference network set construction

In the present study, the GCP is estimated for the ensemble of reference networks, to extract the candidate activated networks in GK and WKY rats. The reference networks are constructed using the binary relationships between transcriptional factors and their regulating genes and the classification scheme for gene function. As for the reference networks, the orthologous genes in rat corresponding all genes in the human binary relationships from TRANSFAC database [13] are first investigated, and then the binary relationships in rat that are composed of the orthologous genes to human are constructed. Based on the binary relationships, transcriptional networks are constructed, according to the functional gene sets previously defined in the Molecular Signatures Database (MSigDB) [14]. In each gene set, the regulated genes in the binary relationships are searched, and if at least one gene is found in the gene set, then the corresponding binary relationships are regarded as a regulatory network characterized by the gene set. The set of constructed networks is used as the reference network for network screening. In present study, the reference network is composed of 1,470 regulatory networks that are constructed from 2,371 transcriptional factor-regulated gene relationships.

Graph Consistency Probability

Network analysis is based on the procedure for estimating the consistency of a network structure (directed acyclic graph) with the measured data for the constituent variables in the graph [11]. First, the joint density function for a given network (reference network) is recursively factorized into conditional density functions according to the parent-descent relationship in the graph [15]. Suppose a causal graph is a directed acyclic graph (DAG), $G(V_i, E_j)$, where V_i is a vertex (i=1, 2, ..., n_v) and E_j is an edge (j=1, 2, ..., n_e) in the graph. The DAG can be factorized into subgraphs according to the parent-descent relationships [15]. Then, the joint density function $f(X_i)$, corresponding to V_i for the graph G, can be factorized into the conditional density functions according to the graph, as follows:

$$f(X_1, X_2, \cdots, X_{n_v}) = \prod_{i=1}^{n_v} f\left(X_i \mid pa\{X_i\}\right), \quad (1)$$

where $pa\{X_i\}$ is the set of variables corresponding to the parents of V_i in the graph.

Second, the causal graph meets the measured data based on the Gaussian graphical model (GN: Gaussian Network) [16]. On the assumption that the probability variable X_i is subjected to a multiple normal distribution, each conditional function in equation (1) is obtained by linear regression for the measured data of the constituent nodes (molecules) measured at m points, i.e.,

$$f\left(X_i \mid pa\{X_i\}\right) = \frac{1}{\sqrt{2\pi\sigma_i^2}} \exp\left[\frac{-1}{2\sigma_i^2}\sum_{k=1}^{m}\left(x_{ik} - \sum_{j=1}^{n_i}\beta_{ij}x_{jk}\right)^2\right], \quad (2)$$

where x_{ik} is the measured value of X_i, at the k-th point, and n_i is the number of variables corresponding to the parents of V_i. Thus, the joint density function in equation (1) is expressed by the regression for the measured data in equation (2). Finally, the logarithm of the likelihood of the equation (2) is calculated for the measured data as

$$l(G_0) = \ln\prod_{i=1}^{n_v} f\left(X_i \mid pa\{X_i\}\right) = -\frac{1}{2}\sum_{i=1}^{n_v}\sum_{j=1}^{n_i}\left\{\frac{1}{\sigma_i^2}\sum_{k=1}^{m}\left(x_{ik} - \sum_{j=1}^{n_i}\beta_{ij}x_{kj}\right)^2 + \ln\left(2\pi\sigma_i^2\right)\right\}. \quad (3)$$

Thus, the GN allows us to quantify a given network into the corresponding numerical value from the measured data, according to the network form. Note that the calculation of likelihood itself requires no assumptions on the relationships between variables. Indeed, the likelihood can be calculated in the case of non-linear regressions, such as spline regression.

Finally, the probability of the log-likelihood for the network structure (graph consistency probability; GCP) is estimated by the distribution of log-likelihoods for many networks generated under the condition that the generated networks shared the same numbers of nodes and edges as those of the given network. In previous paper, we assume that the generated networks follow the extreme value distribution [17]. In this paper, we

generate Nr networks under the same condition, and the GCP is simply defined as

$$GCP = \frac{N_s}{N_r}, \quad (4)$$

where N_r is total number of generated networks, and N_s is the number of networks with larger log-likelihoods than log-likelihood of tested network. In the present study, N_r is set to 2,000. The significance GCP of the given network is set at 0.05 in this analysis.

Enrichment Probability

The network signature is additionally evaluated by the number of constituent genes included in the expression signature. The enrichment probability of the genes in the expression signature for each network is estimated based on the hyper-geometric probability. When the network is composed of k genes, and l genes are detected in the expression signature, then the probability is obtained by

$$P(X \le l) = 1 - \sum_{i=0}^{l} \frac{\binom{M}{i}\binom{N-M}{k-i}}{\binom{N}{k}},$$

where M and N are total number of genes in the expression signature, and total number of genes in the reference networks, respectively.

• Microarray Data

Microarray dataset is cited from the National Center for Biotechnology Information (NCBI) Gene Expression Omnibus (GEO; http://www.ncbi.nlm.nih.gov/projects/geo/) database (GSE 13271). The data are composed of 31,099 probes measured by using Affymetrix Microarray Suite 5.0 (Affymetrix), which are reduced into 14,506 genes, for 5 samples of male Goto-Kakizaki (GK) spontaneously diabetic rats and WKY rats at each of 5 time points (4, 8, 12, 16, and 20 weeks of age). Hyperglycemia begins to show at 4 weeks of age and stabilize after 16 weeks in GK, thus we divided data into three functional groups: 4w, 8-12w, and 16-20w.

Results

• Activated pathways revealed by network screening and their functions

We estimate active regulatory networks among the reference regulatory network set that is generated by the combination of the binary regulatory relationships in TRANSFAC database and the functional gene sets defined in the Molecular Signatures Database (MSigDB). In addition, in each reference network, the enrichment probability of the genes with the significant differences between GK and WKY rats is further tested. Finally, we identify a total of 20 and 19 differentially activating transcriptional regulatory networks in GK and WKY rats, respectively. Table 1 presents detailed significant networks information

Table 1 Identified active regulatory networks in three stages in GK and WKY rats individually. The thresholds of significant pathways in different stages are set to be 0.05.

	GK	*WKY*
4 w	HSC_LATEPROGENITORS_ADULT	HASLINGER_B_CLL_MUTATED NGUYEN_KERATO_UP P21_P53_MIDDLE_DN UVB_NHEK1_C2 VEGFPATHWAY VEGF_HUVEC_30MIN_UP YAGI_AML_PROG_ASSOC ZHAN_MM_CD138_CD1_VS_REST
8-12 w	ATRIA_UP GLYCEROPHOSPHOLIPID_METABOLISM GOLUB_ALL_VS_AML_UP HOHENKIRK_MONOCYTE_DEND_UP HSC_LATEPROGENITORS_ADULT INTEGRINPATHWAY INTEGRIN_MEDIATED_CELL_ADHESION_KEGG LINDSTEDT_DEND_8H_VS_48H_DN LONGEVITYPATHWAY MEF2DPATHWAY P35ALZHEIMERSPATHWAY RCC_NL_UP VHL_NORMAL_UP	ALKPATHWAY BRENTANI_PROTEIN_MODIFICATION CELL_DEATH HCC_SURVIVAL_GOOD_VS_POOR_UP HSC_LATEPROGENITORS_SHARED ICF_UP NI2_LUNG_DN PARK_RARALPHA_MOD SCHURINGA_STAT5A_UP TGFBPATHWAY
16-20 w	ASTON_OLIGODENDROGLIA_MYELINATION_SUBSET BRCA_BRCA1_NEG LEI_HOXC8_DN TESTIS_EXPRESSED_GENES TSADAC_RKOEXP_UP VEGFPATHWAY	NUCLEAR_RECEPTORS

separated by ages and strains. There are fewer pathways activating at 4w and 16-20w in GK rats which are at the beginning and the steady state of diabetes. While during 8-12w, more pathways are significantly activated, which indicates a dynamic process involving dysfunctions and compensations in the development of diabetes, as showed outside blood glucose fluctuations. There are more active pathways in the 4w and 8-12w than those in the 16-20w in WKY, which may be due to body growth and development. It is worth pointing out that many activating pathways in WKY are diminished in GK rats at 4w, suggesting that those pathways in the liver important to keep glucose metabolism homeostasis are dysfunction at very early stages of diseases.

Apart from the view of differentially activated networks along the time points, the networks in the GK and WKY strains can be classified into 4 functional categories in Table 2, which are metabolism, immune, transcription, and signal transduction. Note that some activated pathways share their functions. In that case, they are listed under several functional groups as long as the condition met. Then, we combine the activated networks belonging to the same functional category, if any constituent genes of transcriptional factor (TF) and its regulated gene share each other in the networks. Thus TF-gene expression networks for each functional category are created (Figures 1, 2, 3, 4), where the appearance of sub-networks depending on time points is distinguished by colored nodes and edges. Interestingly, significantly activated networks in GK and WKY strains are very different even in the same functional category. We will describe the details of the activated networks in 4 functional categories, below.

• Metabolism

Metabolic TF regulatory network in WKY rats reveals increased expression of several genes are important to keep metabolic homeostasis, e.g. bone gamma-carboxyglutamic acid-containing protein (BGLAP), Hepatocyte nuclear factor 4 alpha (HNF4A) and Lipoprotein lipase (LPL) (Figure 1A). In addition to its role in bone-building, BGLAP, also known as Osteocalcin, acts as a hormone on metabolic regulation. BGLAP stimulates pancreatic beta cells releasing more insulin and

Table 2 Active regulatory networks classification according to their functions.

	GK	*WKY*
Metabolism	HSC_LATEPROGENITORS_ADULT ATRIA_UP GLYCEROPHOSPHOLIPID_METABOLISM GOLUB_ALL_VS_AML_UP HOHENKIRK_MONOCYTE_DEND_UP HSC_LATEPROGENITORS_ADULT LONGEVITYPATHWAY VHL_NORMAL_UP	HASLINGER_B_CLL_MUTATED VEGF_HUVEC_30MIN_UP YAGI_AML_PROG_ASSOC ZHAN_MM_CD138_CD1_VS_REST
Immune	HSC_LATEPROGENITORS_ADULT LINDSTEDT_DEND_8H_VS_48H_DN LEI_HOXC8_DN TESTIS_EXPRESSED_GENES TSADAC_RKOEXP_UP	NGUYEN_KERATO_UP ICF_UP
Transcription	HSC_LATEPROGENITORS_ADULT ATRIA_UP GOLUB_ALL_VS_AML_UP HOHENKIRK_MONOCYTE_DEND_UP HSC_LATEPROGENITORS_ADULT MEF2DPATHWAY P35ALZHEIMERSPATHWAY	VEGFPATHWAY HCC_SURVIVAL_GOOD_VS_POOR_UP HSC_LATEPROGENITORS_SHARED SCHURINGA_STAT5A_UP NUCLEAR_RECEPTORS CELL_DEATH NI2_LUNG_DN PARK_RARALPHA_MOD NUCLEAR_RECEPTORS TGFBPATHWAY
Signaling Transduction	INTEGRINPATHWAY INTEGRIN_MEDIATED_CELL_ADHESION_KEGG MEF2DPATHWAY P35ALZHEIMERSPATHWAY RCC_NL_UP VHL_NORMAL_UP ASTON_OLIGODENDROGLIA_MYELINATION_ SUBSET BRCA_BRCA1_NEG LEI_HOXC8_DN TESTIS_EXPRESSED_GENES TSADAC_RKOEXP_UP VEGFPATHWAY HSC_LATEPROGENITORS_ADULT	P21_P53_MIDDLE_DN UVB_NHEK1_C2 ALKPATHWAY BRENTANI_PROTEIN_MODIFICATION CELL_DEATH NI2_LUNG_DN PARK_RARALPHA_MOD TGFBPATHWAY NUCLEAR_RECEPTORS

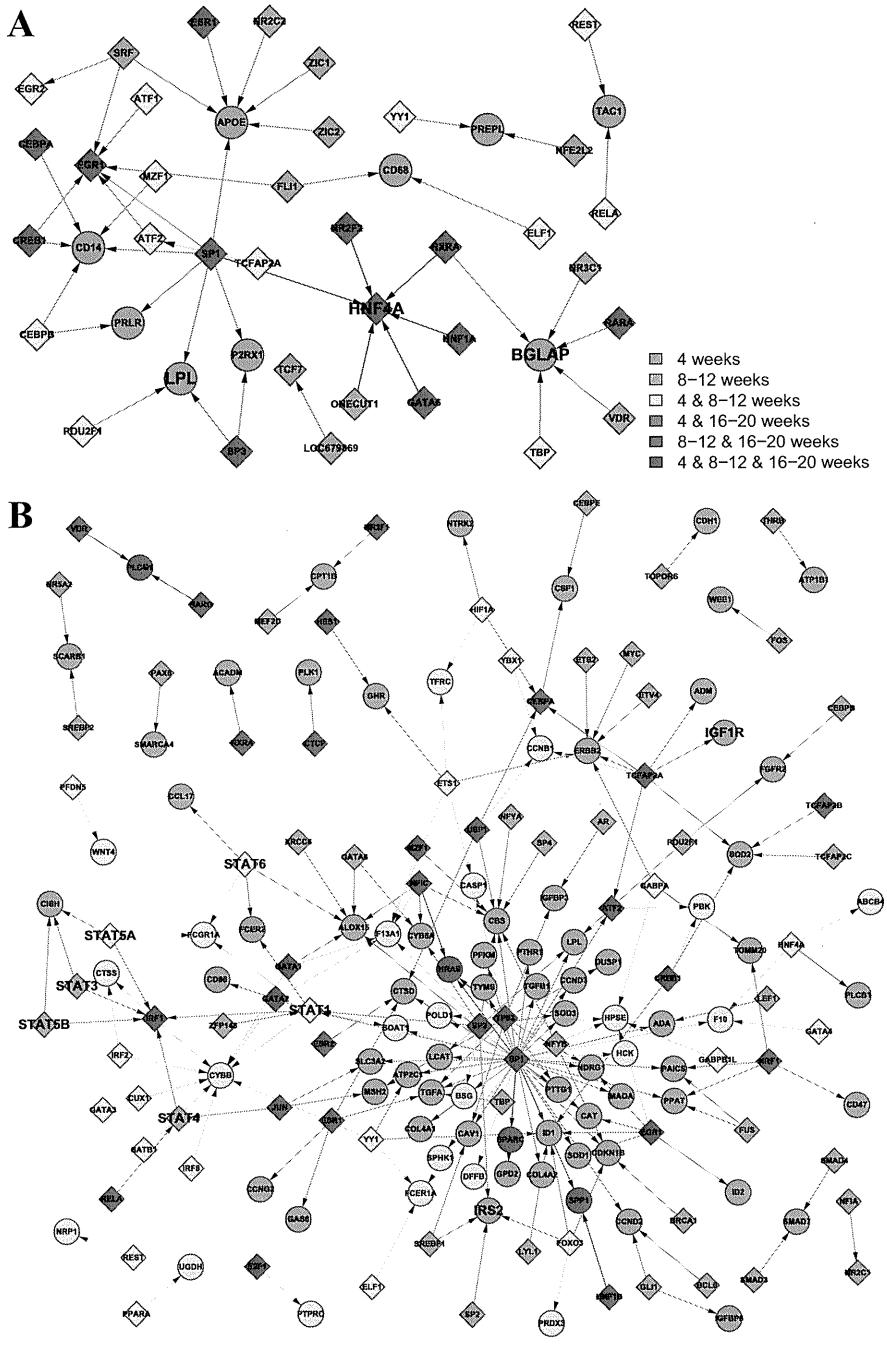

Figure 1 Combined networks in the metabolic functional category. TF-gene expression graphs in WKY and GK strains are displayed in subfigure A and B, respectively. TF and regulated genes are shown in diamonds and circles, respectively. Selected molecules as the examples to explain in this paper are shown in bigger font. The appearance of each sub-network at time points is distinguished by colored nodes and edges in the following ways: 4w, gray; 4w and 8w-12w, yellow; 4w and 16w-20w, purple; 4w, 8w-12w, and 16w-20w, red; 8w-12w, right blue; 8w-12w and 16w-20w, blue; and 16w-20w, green.

increases insulin sensitivity via enhancing adipocytes adiponectin secretion [18]. HNF4A plays a key role in liver development. Mutations in this gene have been associated with maturity-onset non-insulin-dependent diabetes of the young (MODY) [19]. Our analysis indicates that reduced HNF4A expression may also favor T2DM development in GK rats. LPL is an enzyme that hydrolyzes triglyceride in lipoproteins such as very low-density lipoproteins (VLDL) and reforms high-density lipoproteins (HDL). Lipoprotein lipase deficiency

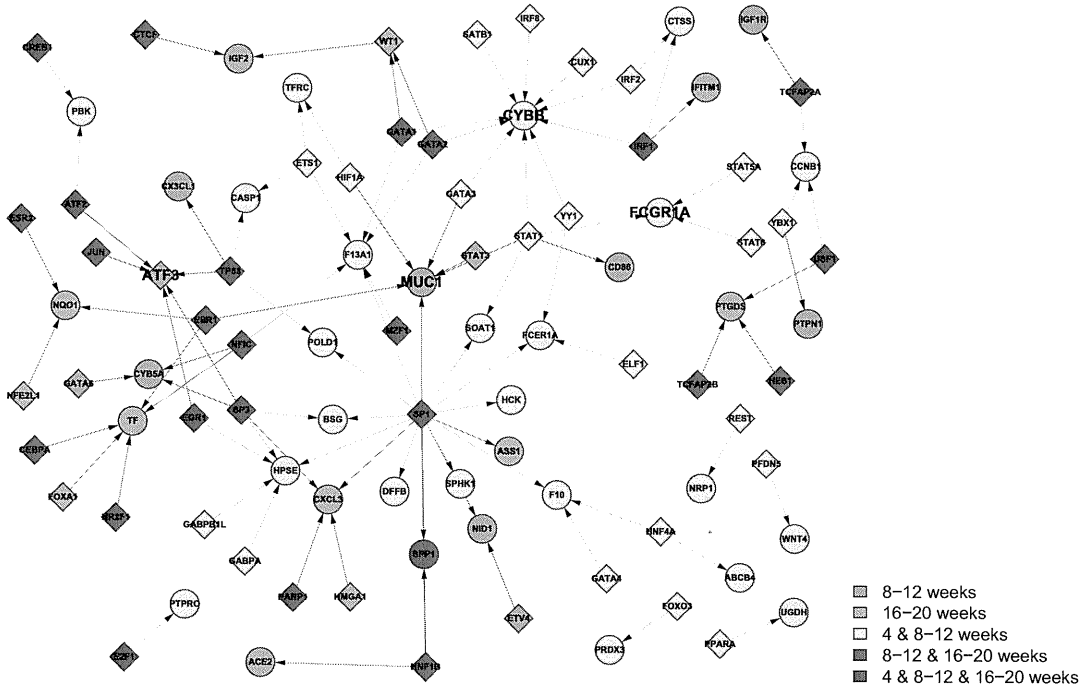

Figure 2 Combined networks in the immune functional category in GK rat. The appearance of each sub-network at time points is distinguished by the same way as Figure 1. Many proinflammatory related pathways active comparing GK to WKY rats. There are two hubs CYBB and ATF2 that play important role in immune damages observed in GK.

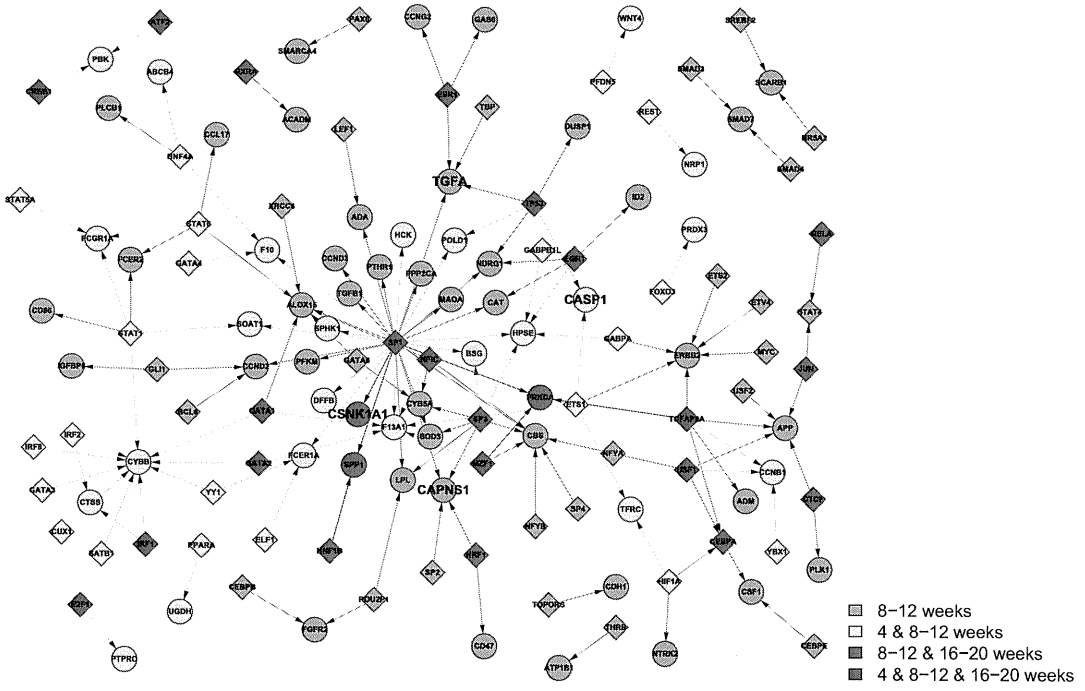

Figure 3 Combined networks in the transcription functional category in GK rat. The appearance of each sub-network at time points is distinguished by the same way as Figure 1. This graph highlights genes causing apoptosis and neurodegenerative disorders, such as Alzheimer's disease.

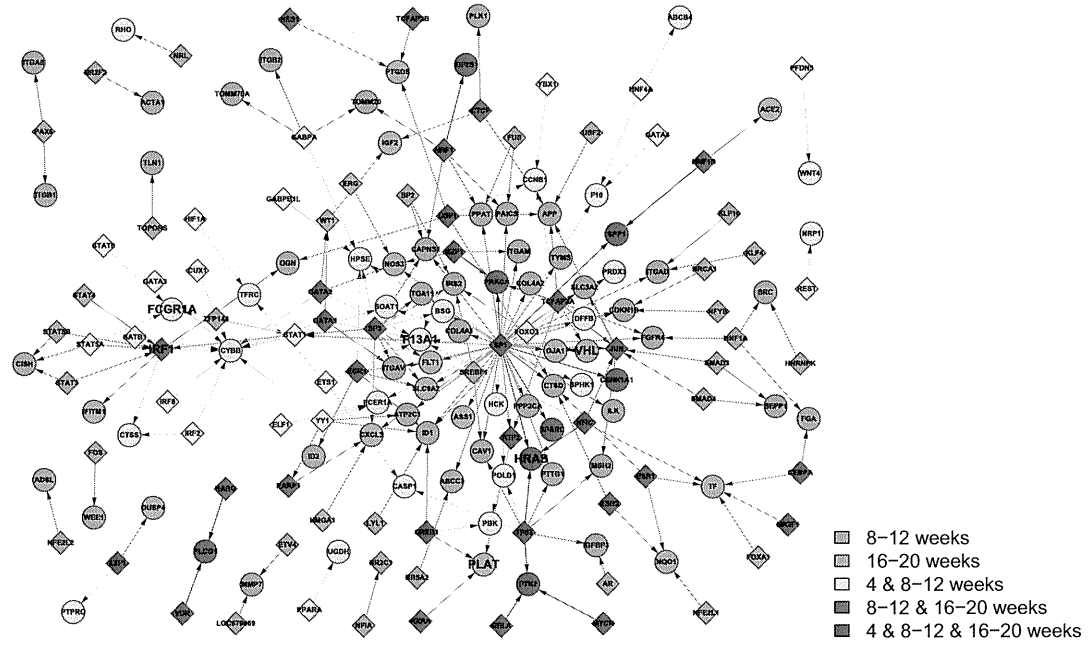

Figure 4 Combined networks in the signal transduction functional category of GK rats. The appearance of each sub-network at time points is distinguished by the same way as Fig. 1. Activation of hypoxia and coagulation related pathways is the key difference between GK and WKY strains.

leads to elevated levels of triglycerides in the bloodstream. Increment of LPL activity leads to decreased triglycerides levels, elevated HDL levels, a significant fall in fasting glucose and glycohemoglobin, and delayed complication occurrence [20]. Interestingly, like HNF4A, LPL is also suggested to be a diabetes susceptibility gene by human studies [21].

Metabolic networks in GK rats are more complicated than those in WKY rats (Figure 1B). Besides the reduced expression of three genes described in the previous paragraph in diabetic GK rats, some pathways identified by network screening further contribute to metabolism disorders. Several signal transducers and activators of transcription (STATs) are found in GK TF regulatory metabolic network. Diabetic GK rats are reported to have higher levels of Cytokines [12]. Cytokines induce activation of janus kinase (JAK)-STAT pathway leading to expression of various suppressors of cytokine signaling (SOCS) (not shown in the figure). Checking original microarray data we found that expression of SOCS2 and STAT5 but not SOCS3 is decreased in GK rats. Decreased expression of SOCS2 leads to enlarged internal organs, which consists with the description in the original paper that liver weight as a percentage of total body weight is significantly larger in GK [12,22,23]. Insulin directly stimulates SOCS2 and STAT5 expression, and the decreased SOCS2 and STAT5 levels are due to insulin deficiency or resistance. Beta cell mass after birth is only half in GK compared to WKY rats. The higher plasma insulin levels in GK measured via Millipore RI-13K rat insulin RIA kit may be due to cross reaction with elevated proinsulin. At later stage, insulin resistance also occurs. IGF-1 (insulinlike growth factor-1) has a function similar to insulin, and it can also improve blood sugar profiles in type 2 diabetics. IGF-1 deficiency mice were very insulin insensitive, while administration of IGF-1 shows the insulin resistance improvement [24]. IGF-1 levels are increased at 4w, but significantly decreased, thereafter. While IGF1 receptor (IGF1R) is exclusively down-regulated, decreased IGF1R signaling pathway may partially explain the insulin resistance after 8 weeks of age in GK rats.

We also observed some compensative pathways activation in GK to fight against insulin resistance. For instance, insulin receptor substrate 2 (IRS2) is up-regulated and SOCS1 is down-regulated at 8-12w. Cytokine-induced SOCS-1 interacts with the phosphorylated insulin receptor and promotes ubiquitination (Ub) and degradation of IR-IRS complex, thereby preventing insulin signaling pathways [25]. Decreased SOCS-1 is correlated to insulin sensitivity. However, compensations fail to stop development of diabetes.

- **Immune**

Many proinflammatory pathways are activating in GK compared to WKY rats (Figure 2). From the TF-

regulatory gene expression networks in GK rats, two hubs which play important role in immune damages are displayed.

Cytochrome b-245, beta polypeptide (CYBB) is a gene encoding gp91(phox) protein, a phagocyte NADPH oxidase. The protein is also known as P91-PHOX and NOX2. Reactive oxygen species (ROS) produced by NOX2 are able to kill phagocytized bacteria. Because of its highly reactive nature, CYBB has been considered harmful mediators of inflammation [26]. NF-KB and interferon-gamma further increase CYBB expression. Prolonged highly CYBB expression enhanced production of reactive oxygen species, which are critical sources mediating neurovascular damage. Significantly overexpressed CYBB in GK stain is a critical contributor to the microvascular complications associated with diabetes.

Activating transcription factor 3 (ATF3) is a stress-inducible gene and encodes ATF3 transcription factors. ATF3 expression has been reported up-regulated in insulitis and type 1 or type 2 diabetics. Induction of ATF3 is mediated by proinflammatory factors, such as nitric oxide and NF-κB. Importantly, the induction of ATF3 leads cell apoptosis, while signals without ATF3 up-regulation do not cause cell damage [27]. Increased gene expression of ATF3 in GK rats are related to increased immune response and apoptosis.

Besides these two hubs, about 20 immune related genes are changed in GK strain. Some are up-regulated, such as high affinity immunoglobulin gamma Fc receptor I (FCGR1A). Some are down-regulated, such as cell surface associated (MUC1), which protects the body from infection by binding to pathogens. In sum, inflammation is significantly increased in diabetic Gk rats.

• Transcription

Pathways analysis reveals that WKY transcriptional network is a balanced and well-controlled system. Several pathways (VEGFPATHWAY, HCC_SURVIVAL_GOOD_VS_POOR_UP, HSC_LATEPROGENITORS_SHARED, SCHURINGA_ STAT5A_UP) are involved in cell replication, good survival and self renewal. Others, including P21-P53_Middle_DN, UBV_NHEK1_C2, and TGFBPATHWAY, emphasize anticancer and cell cycle checkpoints regulation (Table 2).

In GK rats, two out of 7 pathways are related to apoptosis (Table 2 and Figure 3). Caspase 1 (CASP1), which has been shown to induce cell apoptosis, is overexpressed. Transforming growth factor alpha (TGFA), which stimulates neural cell proliferation, is inhibited. Interestingly, diabetes activates several genes involving in neurodegenerative disorders. Alzheimer's disease shares many commons with T2DM, so that some scientists proposed to call Alzheimer's disease "type 3 diabetes" or "diabetes of the brain." Calpain small subunit 1 (CAPNS1), a highly-conserved cysteine protease, which have been implicated in neurodegenerative processes after oxidative stress stimulation, is more active in GK. Casein kinase I isoform alpha (CSNK1A1), also called CK1α, is associated with phosphorylate tau and amyloid formation [28]. Reduction in CK1α expression induces Tau phosphorylation inhibition. The expression of CK1α gene is much higher in GK.

• Signal transduction

The key difference in signal transduction category is activation of hypoxia and coagulation related pathways in GK rats (Table 2 and Figure 4). Coagulation factor XIII A chain (F13A1) is the last zymogen activating in the blood coagulation cascade, which stabilize clots [29]. In GK rats, F13A1 gene expression levels are significantly elevated which enhance thrombosis. Macrophages expressing high affinity immunoglobulin gamma Fc receptor I (FcgRIa) also display coagulation function via binding platelets and initiate thrombosis. [30]. Tissue plasminogen activator (PLAT) breakdowns blood clots. GK rats present significantly higher PLAT expression levels, which may explain hemolysis and thrombosis co-existing in diabetics. Dr. Auwerx reported in diabetics, PLAT and plasminogen activator (PA) inhibitor are both activated [31]. The elevated levels of PA-inhibitor activity abolish PLAT activity inducing a reduced fibrinolytic capacity.

RCC_NL_UP and VHL_NORMAL_UP are two networks involved in hypoxia. The von Hippel-Lindau tumor suppressor -hypoxia-inducible factor (VHL-HIF) pathways are key players in tumor hypoxia survival. Many genes involved in such pathways include interferon regulation factor 1(IRF 1), GTPase HRas (HRAS), and VHL, are negatively expressed in GK strain. T2DM shows increased incidence and delayed recovery from hypoxia. Reduced hypoxia network activity potentially plays a pivotal role in this phenomenon.

• Dynamic changes of regulatory networks

In order to understand the dynamical changes of regulatory networks in the development of diabetes, we drew the active networks at each time segments (Figures 5, 6, 7). Among the genes in the networks, some can be seen in more than one time segment, which are considered to be more important than others, and are distinguished by the colored nodes and edges according to their appearance in which time segments. Furthermore, the information on the expression degree is also important in comparison with GK and WKY, and is indicated in the node form in each network.

At the beginning of hyperglycemia, TF regulatory network in 4w GK displays 12 genes differently expressed between GK and WKY (Figure 5). Those genes can be